INTERNATIONAL CONFERENCE ON ENGINEERING DESIGN
ICED 03 STOCKHOLM, AUGUST 19-21, 2003

OPTIMAL DESIGN OF A LIGHTWEIGHT SHAPE MEMORY ALLOY ACTUATOR

L. H. Han[*], T. J. Lu[*], and A. G. Evans[**]

Abstract

A minimum weight flexural actuator comprising a triangular truss core and Shape Memory Alloy (SMA) actuation elements is designed. The two-way actuation element design is described. The actuation force and strain of SMA actuation elements are obtained by solving a coupled problem that combines a thermomechanical constitutive model of SMAs, heat conduction equation and the spring response. The optimal algorithms are developed to obtain the optimal design parameters and the minimum weight, subject to multiple nonlinear constraints.

Keywords: optimisation design, sensors and actuators, thermomechanical processes

1 Introduction

Statically determinate structures with truss elements have simple mechanisms, light weight and high rigidity [1,2,3]. They are suitable for adaptive structures that can achieve uniform strains without energy lost by actuating a subset of the truss. Lu et al. [4,5] have presented the optimal design of high authority flexural actuators comprising a passive triangular truss core and two active faces. They pointed out that the statically determinate truss design with frictionless-pinned joint did not store elastic energy and power when the faces are actuated alternatively. However, in their design, the actuation element (one face) cannot automatically recover to its original position after actuated, and its recovery depends on the actuation of the other. As an extension of this work, the design of a modular SMA actuation element that can automatically implement the actuation-recovery cycle is proposed in this study.

2 Design of SMA actuator

2.1 Design concept

The basic concept is a lightweight actuator with actuation elements and a corrugated core. The actuator has the same geometry and boundary conditions as described in Lu et al. [4], except that the top surface is replaced by a series of SMA actuation elements (Fig. 1). It is required to flex over a displacement against restraining springs and dashpots modelled as a constant force,

[*] Engineering Department, University of Cambridge, Cambridge, CB2 1PZ, UK
[**] Materials Department, University of California, Santa Barbara, CA93106, USA

which may vary with displacements and frequencies. The actuation elements are assembled with the corrugated core by frictionless-pinned joints on the top surface. The corrugated core is free of rotational resistance. In addition, it provides negligible resistance to the stretching and contractions of the SMA actuation elements as they actuate. An activated SMA actuator is shown in Fig.2.

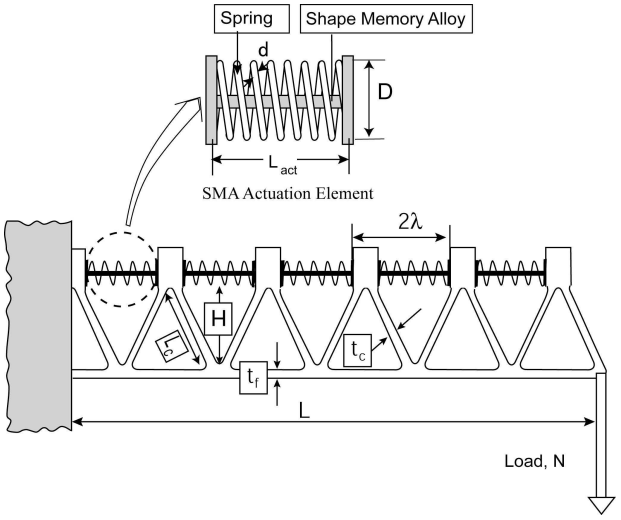

Figure 1. The flexural structure with actuation elements

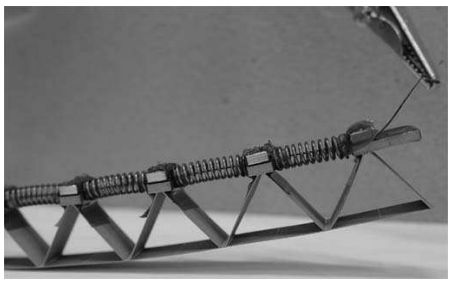

Figure 2. Activated SMA actuator

2.2 Operation principle

As shown in Fig.1, the SMA actuation element consists of an one way SMA wire and a bias compressive spring which makes the structure work in a two-way manner. When the SMA wire is heated to the finish temperature for the austenite transformation, the recovery force generated by the shape memory effect (SME) will compress the spring so as to store energy in the spring. When the SMA actuator is cooled down to the martensite finish temperature, the potential energy stored in the bias spring will be released to strain the SMA wire back to its initial position, resulting in a deformation-reformation cycle.

The design of SMA actuation elements is given in Fig. 3. The stress-strain curves are the thermomechanical response of the SMA at different temperatures. The straight line 1 represents the spring response.

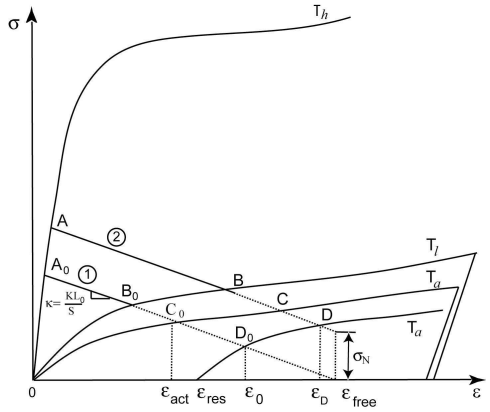

Figure 3. SMA actuation element design concept

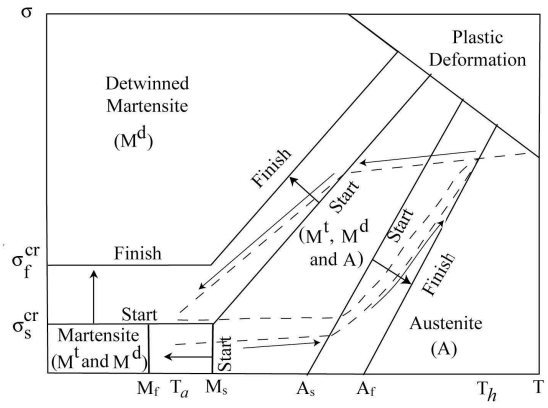

Figure 4. Critical stress-temperature diagram for SMA transformation

If there is no external force, when the SMA actuator is electrically heated from T_l to T_h, the spring is compressed from point B_0 to A_0; then the current is cut off and cooled to T_l, the spring is released from point A_0 to B_0. If an external force F_N (stress σ_N) is applied, the work line A_0B_0 displaces to AB. As a practical matter, T_h is chosen to be the austenite finish temperature; T_l is chosen to be the martensite finish temperature. The transformation temperatures, austenite start A_s, austenite finish A_f, martensite start M_s, and martensite finish M_f, are functions of the stress. The larger the stress is applied, the higher the temperature that will be required to start and finish the transformation of the austenite and martensite phases. The transformation temperatures can be determined from the critical stress-temperature diagram of SMA transformation (Fig.4). In Fig. 4, the dash lines show the stress and temperature change of the SMA wire during the heating and cooling cycle of the actuation element between T_a and T_h (Fig.3).

To predict the unique thermomechanical behaviour of SMAs at all temperatures, Brinson's constitutive model [6] with non-constant material properties is used in this study. Generally, the constitutive equation can be expressed as

$$\sigma - \sigma_0 = E(\xi)\varepsilon - E(\xi_0)\varepsilon_0 + \Omega(\xi)\xi_s - \Omega(\xi_0)\xi_{s0} + \Theta(T - T_0) \tag{1}$$

where σ, ε, T and ξ represent the stress, strain, temperature and martensite fraction, respectively. $E(\xi)$ is the modulus of the material, $E(\xi) = E_A + \xi(E_M - E_A)$, Θ the thermal coefficient of expansion, and $\Omega(\xi)$ the transformation tensor, $\Omega(\xi) = -\varepsilon_L E(\xi)$. ε_L is the maximum recoverable strain, E_A and E_M are the Young's modulus at the martensite and austenite states. The subscript "0" denotes initial conditions. ξ and ξ_s are defined by phase transformation kinetic equations as functions of temperature and effective stress in the SMA. The transformation kinetics equations are given in the reference [6].

The stress-strain relation of the spring (straight line 1 in Fig. 3) can be presented as

$$\sigma - \sigma_0 = -\frac{KL_0}{S}(\varepsilon - \varepsilon_0) = -\bar{K}(\varepsilon - \varepsilon_0) \tag{2}$$

where K, L_0 and S are the spring rate, initial length and cross-sectional area of the SMA wire; $\bar{K} = \frac{KL_0}{S}$ is the normalised spring rate. The larger the normalised spring rate $\bar{K}$, the higher the resulting recovery stress σ.

Based on Eqs.(1) and (2), the thermomechanical response of the SMA actuation element can be simulated quantitatively.

2.3 Problem definition

The objective is to design an actuator capable of realizing a specified performance (authority) at the lowest possible overall weight, given by:

$$W = \rho_f LBt_f + \rho_c \left[\frac{L}{\cos\beta}\right] Bt_c + N_m\left(W_{SMA} + W_{Spring}\right) \tag{3}$$

where ρ_f and ρ_c are the densities of the lower face sheet and core materials, $W_{SMA} + W_{SMA}$ is the weight of the actuation element (above) and $N_m = (L - \lambda)/2\lambda$ is the total number of

actuation elements. The design problem addresses temperatures, power requirements, failure mechanisms, displacements and operational frequency etc.

The following definitions are used. The lower face sheet has thickness t_f, length L, width B; the core has thickness t_c, height H, pitch length 2λ and corrugation angle $\beta = 54.7^o C$. The SMA wire has diameter r, density ρ_{SMA}.

3 Design considerations

3.1 Actuation strain

Upon heating, the strain experienced by the actuation element is the sum of three contributions: elastic strain due to stress, thermal expansion and phase transformation. It can be derived from Eqs. (1) and (2), as:

$$\varepsilon = -\left[\bar{K} + E(\xi)\right]^{-1}\left[-E\left(\xi_0\right)\varepsilon_0 + \Omega(\xi)\xi_s - \Omega(\xi_0)\xi_{s0} + \Theta\left(T - T_0\right)\right] \tag{4}$$

If the actuation element is heated from T_l to T_h (Fig.3), the total actuation strain $\varepsilon_T = \varepsilon_{B_0} - \varepsilon_{A_0}$ when no external force is applied. ε_{A_0} and ε_{B_0} can be calculated from Eq. (4).

3.2 Transient response of SMA actuators

The SMA wire is resistively heated and cooled by convection. The governing equation for the 2D heat conduction problem of a SMA wire [7] is

$$\rho c_p \frac{\partial T}{\partial t} = k\left(\frac{\partial^2 T}{\partial r^2} + \frac{1}{r}\frac{\partial T}{\partial r}\right) - \frac{2h}{r}\left(T - T_0\right) + \rho_e\left(\frac{I^2}{\pi r^2}\right) \tag{5}$$

where T is the temperature at the location (x, r) at time t, x is along the length direction; r is the radius direction. The constants c_p, ρ, k, h, ρ_e, T_a and I are the heat capacity, density, thermal conductivity, heat transfer coefficient (natural convection), electric resistivity, ambient temperature and electric current, respectively. The finite element codes in Matlab have been developed to solve this differential equation. Figure 5 shows the temperature distribution of the SMA wire along its radius and axial directions when the electrical current is applied. Note that when the wire diameter is small, the temperature distribution in the radial direction is almost uniform. Therefore, for simplicity, the temperature distribution obtained with the 1D model analysis can be used [4].

For the heating process, the temperature response of the wire can be expressed as

$$T - T_a = T_0\left(1 - e^{-\frac{t}{\tau}}\right) \tag{6}$$

where $T_0 = \dfrac{I^2 R}{2\pi r h} = \dfrac{P}{2\pi r h}$ is the final stable state temperature, $\tau = r\rho c_p/(2h)$; P is the power supplied to the actuator and R is the resistance of the wire ($R = \rho_e L_{wire}/S$), where L_{wire} is the wire length. In the design, the power supply has a specified upper limit, P_0.

For the cooling process, the temperature response of the wire can be expressed as

$$T - T_a = (T_h - T_a)e^{-\frac{t}{\tau}} \tag{7}$$

where T_a is the ambient temperature, and T_h is the temperature at the beginning of cooling

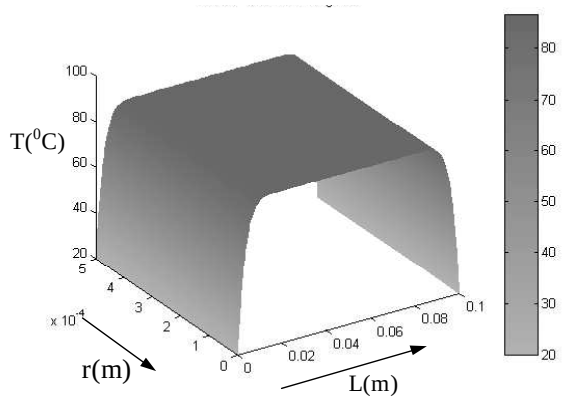

Figure 5. The temperature distribution of the SMA wire

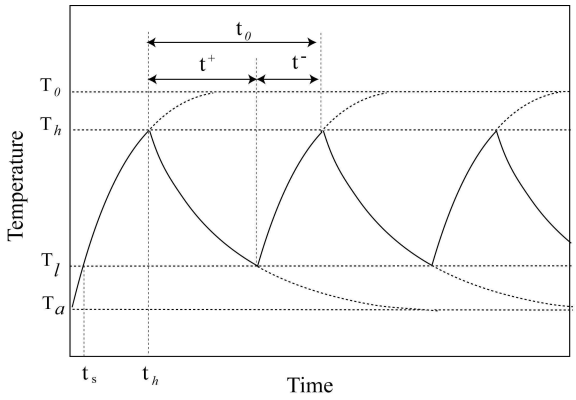

Figure 6. Heating and cooling cycles of SMA wires

From Eqs (6) and (7), the cycle time t_0 as shown in Fig. 6 can be derived as

$$t_0 = t^+ + t^- = \frac{r\rho c_p}{2h} \ln\left(\frac{T_0/(T_l - T_a) - 1}{T_0/(T_h - T_a) - 1}\right) \tag{8}$$

where t^+, t^- and T_l are the heating time, cooling time and temperature at the end of cooling.

The operational frequency of the SMA actuation element becomes

$$f \equiv \frac{1}{t_0} \tag{9}$$

3.3 Spring design

To minimize the total weight of the actuation system, the weight of the spring should also be minimized. The weight of the spring is given by [8]:

$$W_{Spring} = \left[\frac{\pi^2}{4}\right]\rho_s d^2 D\left[\frac{N_a}{\cos\theta} + N*\right] \tag{10}$$

where ρ_s is the density of the spring wire, D is the mean diameter of the spring, d is the coil diameter, and θ is the helix angle (the angle between the coils and the base of the spring). Here N_a and N^* are the number of active and inactive coils, respectively. The helix angle θ is related to the coil-pitch $\bar{p}$ by: $\theta = \tan^{-1}(\bar{p}/\pi D)$. A closed-coil requires a small helix angle ($\theta \le 15^o$), therefore $\cos\theta \approx 1$. For plates in contact with the end of the spring, $N^* = 2$. The number of active springs, N_a, is governed by the spring constant as: $N_a = Gd^4/8D^3K$, with G the shear modulus of the wire, such that, from (10):

$$W_{Spring} \approx \left(\frac{\pi^2}{4}\right)\rho_s d^2 D\left[\frac{Gd^4}{8D^3K} + 2\right] \tag{11}$$

High strength steel wires are chosen for lightweight springs [9]. The maximum compression of the spring occurs in the actuation element located at the clamped end of the actuator. It is given by Point A_0 in Fig. 3:

$$\Delta_{\max} = L_0 \left(\varepsilon_{free} - \varepsilon_{A_0} \right) \tag{12}$$

where $\varepsilon_{free} = \left(L_{free} - L_0 \right) / L_0$, and L_{free} is the free length of the spring.

Besides the geometry constraints, such as the lowest limit on the number of coils, the limited spring index, the size of mean diameter and the wire diameter etc., failure criteria of the spring, such as yielding, buckling, fatigue and surging, should also be considered [8].

3.4 Failure criteria of passive structure

Since the actuation itself does not induce significant stress (given the static determinancy), the failure mechanisms of the passive structure are activated by the resistive external load. In considering the strength, three failure modes of the structure may occur: namely, face yielding, core yielding and core buckling. The detailed analysis can be found in [5].

3.5 End deflection

Upon heating, the total length of the actuation elements on the top face is reduced by $\Delta L = -\varepsilon_T L$, where ε_T can be calculated from Eq. (4). The structure bends upwards, with the tip deflection due to the combined effect of SMA contraction and thermal expansion, δ_1, given by

$$\delta_1 = H\left(\frac{1}{2} + \frac{L}{\Delta L} \right)\left(1 - \cos\frac{\Delta L}{H} \right) \tag{13}$$

The tip deflection δ_2 due to a resistance N imposed at the free end is [10],

$$\delta_2 = \frac{1}{3}\frac{NL^3}{D_{eq}} + \frac{NL^2}{D_q} \tag{14}$$

where the equivalent flexural stiffness D_{eq} may be derived according to the beam theory [11], D_q is the transverse shear stiffness [4]. Accordingly, the tip deflection, $\delta = \delta_1 - \delta_2$, with $\delta \geq \delta_0$ required.

4 Optimisation design

4.1 Formulation of the optimisation problem

The optimisation problem for minimum weight can be summarized using non-dimensional variables. The initial goal is to minimize the actuator weight given in non-dimensional form by

$$\Psi = \frac{W}{\rho_f BL^2} = w_{face} + w_{core} + w_{SMA} + w_{spring} \tag{15}$$

where

$$w_{face} = \frac{t_f}{L} \tag{16}$$

$$w_{core} = \frac{1}{\cos\beta}\frac{\rho_c}{\rho_f}\frac{t_c}{L} \tag{17}$$

$$w_{SMA} = 0.5\left(\frac{L}{H}\tan\beta - 1\right)\pi\frac{\rho_{SMA}}{\rho_f}\left(\frac{L_{act}}{L}\right)\frac{L}{B}\left(\frac{r}{L}\right)^2 \tag{18}$$

$$w_{spring} = 0.5\left(\frac{L}{H}\tan\beta - 1\right)\frac{\pi^2}{4}\frac{\rho_s}{\rho_f}\left(\frac{d}{L}\right)^2\left(\frac{D}{L}\right)\frac{L}{B}\left(\frac{N_a}{\cos\theta} + 2\right) \tag{19}$$

The weight minimization is subject to the following constraints:

$$1 - \left(\frac{1}{2} + \frac{1}{\varepsilon_T}\right)\frac{H}{L}\left(1 - \cos\varepsilon_T\frac{L}{H}\right)\frac{\delta_0}{L} + \frac{1}{3}\left[\frac{N}{E_f BL}\right]\frac{B}{L}\left(\frac{E_f L^4}{D_{eq}}\right)\frac{\delta_0}{L} + \frac{\delta_0}{L}\left[\frac{N}{E_f BL}\right]\frac{E_f L^2}{D_q} \le 0 \quad \text{(Minimum deflection)} \tag{20}$$

$$\frac{B}{L}\left(\frac{L}{t_f}\right)\left(\frac{L}{H}\right)\left[\frac{N}{E_f BL}\right]\frac{E_f}{\sigma_Y^f} - 1 \le 0 \quad \text{(Face yielding)} \tag{21}$$

$$\frac{1}{\sin\beta}\left[\frac{N}{E_f BL}\right]\frac{E_f}{\sigma_Y^c}\left(\frac{L}{t_c}\right) - 1 \le 0 \quad \text{(Core yielding)} \tag{22}$$

$$\frac{12}{\pi^2\sin^3\beta}\left[\frac{N}{E_f BL}\right]\frac{E_f}{E_c}\left(\frac{L}{t_c}\right)^3\left(\frac{H}{L}\right)^2\left(\frac{(\pi^2 C_A + 2)(\pi^2 C_B + 2)}{(\pi^2 C_A + 4)(\pi^2 C_B + 4)}\right) - 1 \le 0 \quad \text{(Core buckling)} \tag{23}$$

There are multiple constraints for the actuating element:

$$1 - \frac{1}{48(1+\nu)}\left[\frac{E_f L}{K}\right]\left(\frac{L}{D}\right)^3\left(\frac{d}{L}\right)^4\frac{E_S}{E_f} \le 0 \quad \text{(Minimum number of coils)} \tag{24}$$

$$(D/L)(L/d)/20 - 1 \le 0 \quad \text{(Upper Limits on spring index)} \tag{25}$$

$$1 - (D/l)(L/d)/4 \le 0 \quad \text{(Lower Limits on spring index)} \tag{26}$$

$$\frac{\Delta_{\max}}{L} \le 0.91\left[\frac{L_{free}}{L} - \frac{d}{L}(N_a + 3)\right] \quad \text{(Clash allowance)} \tag{27}$$

$$1 - \frac{1}{6\pi N_a f_{an}}\frac{d}{D^2}\sqrt{\frac{Gg}{32\rho_s}} \le 0 \quad \text{(Surging)} \tag{28}$$

$$1 - \frac{L_{free}}{(1+\varepsilon_T)L_{act}} \le 0 \quad \text{(Spring compression)} \tag{29}$$

$$1 - \frac{\varepsilon_{\max}}{0.05} \le 1 \quad \text{(Maximum working strain of the SMA wire)} \tag{30}$$

$$T_h/T_{\max} - 1 \le 0 \quad \text{(Maximum allowable heating temperature of the SMA wire)} \tag{31}$$

$$1 - f/f_0 \le 0 \quad \text{(Operational frequency)} \tag{32}$$

$$P/P_0 - 1 \le 0 \quad \text{(Power requirement)} \tag{33}$$

Structural integrity of the spring

$$1 - \frac{S_{es}(S_{us} - \tau_i)}{S_{es}(\tau_m - \tau_i) + S_{us}\tau_a} \le 0 \quad \text{(Fatigue)} \tag{34}$$

$$8K_s\left[\frac{K}{\pi E_f L}\right]\left(\frac{\Delta_{\max}}{L}\right)\frac{D}{L}\left(\frac{L}{d}\right)^3\frac{E_f}{S_{ys}}-1\le 0 \qquad \text{(}\textit{Yielding}\text{)} \qquad (35)$$

$$\left[1+\left[4.26\frac{D}{\Delta_{\max}}\left(\frac{D}{L}\right)\right]^2\right]^{-1}\frac{L_{free}}{L}\left(\frac{L}{\Delta_{\max}}\right)-0.615\le 0 \qquad \text{(}\textit{Spring buckling}\text{)} \qquad (36)$$

The non-dimensional design variables are the face sheet thickness t_f / L, core thickness t_c / L, core height H / L, spring rate $K / E_f L$, mean diameter D / L and wire diameter d / L, and SMA wire diameter r / L.

A Matlab program using the sequential quadratic programming (SQP) approach was implemented to find optimal solutions. Since the objective function has many local optima, an algorithms [12] based on the systematic placement of points was also implemented to generate starting points to optimise the dispersion of the set.

4.2 Design examples

Actuators made with a high strength aluminium alloy are chosen for the design examples. The material properties used are summarized in Table 1.

Table 1. Material Properties of the SMA Wire Used in Simulation

Parameter	Symbol	Unit	Value
Transformation Temperatures [*,**]	M_f	^oC	9
	M_s	^oC	18.4
	A_s	^oC	34.5
	A_f	^oC	49
Young's Modulus[*]	E_M	GPa	26.3
	E_A	GPa	67
Slope of stress* versus temperature plot	C_M	$MPa\,^oC^{-1}$	8
	C_A	$MPa\,^oC^{-1}$	13.8
Thermalelastic coefficient	Θ	$MPa / ^oC$	0.55
Electrical Resistivity	ρ_e	$\Omega\ m$	102.0×10^{-8}
Specific Heat	C_p	J / kg	500
Density	ρ_{SMA}	kg / m^3	6.45×10^3
Poisson's ratio	ν	-	0.33
Maximum transformation strain of SMA	ε_L	-	6.3%
Critical Stress for martensite twin conversion[**]	σ_s^{cr}	MPa	100
	σ_f^{cr}	MPa	170

[*] 'A' and 'M' represent austenitic and martensitic phases, respectively

[**] Subscripts 's' and 'f' represent start and finish temperature

The design parameters are $L = 100mm$, $B = 10mm$, $\varepsilon_T = 0.05$, $\delta_0 / L = 10\%$. The lowest weight $\Psi_{\min}$ and the associated dimensions ($t_f / L, t_c / L, D / L$, d / L and r / L) are determined (Fig. 7).

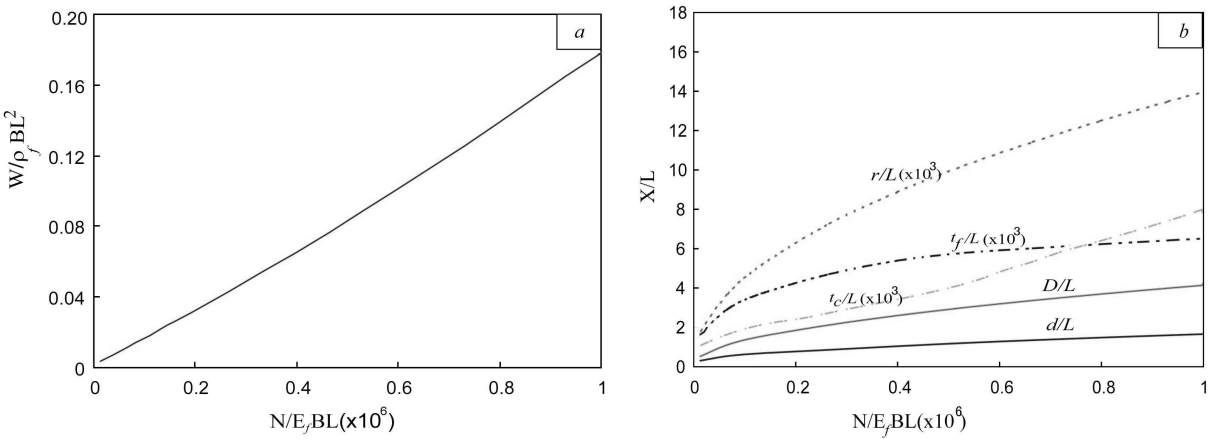

Figure 7. (a) Minimum weight and (b) the associated dimensions plotted as functions of load index $\Pi = N / E_f BL$

With increasing external load, the lowest weight of the actuator increases, accompanied by the increase of the thickness of the bottom surface sheet and the core.

Based on the optimal design analysis, an SMA-based actuator is manufactured (Fig. 2). Both facesheet and core of the passive structure are 0.2 mm thick. The SMA actuation element consists of a 0.375 mm Flexinal SMA wire and a steel compression spring. The total mass of the actuator is 9 grams. A 200 g dead weight is lift to 10 mm high by the actuator, approximate 10% of the total actuator length. The actuator can operate at 0.1 Hz.

5 Discussion and Conclusion

The spring rate is the key to design the SMA actuation element. The larger the spring rate, the higher the temperature that will be required to finish the phase transformation, and the longer the cooling time.

The operational frequency is largely limited by the efficiency of cooling. This frequency can be increased by reducing the wire diameter, or by increasing the heat transfer coefficient. In this design, this may be achieved by using multiple actuation elements in parallel on the top surface.

An optimisation method based on the SQP programming has been developed to analyse the optimum design of the actuator. It shows that the actuator can be designed to operate against large restraining moments at relatively low weight. The triangular corrugation is attractive because of its minimal rotational/bending resistance and high transverse shear stiffness: whereupon the core remains unstressed as the SMA actuation element contracts due to phase transformation. The temperature history is obtained by solving the heat conduction equation in the SMA actuator heated resistively. Coupling the thermomechanical constitutive model with the structural analysis, it is possible to predict the behavior of the actuator by using temperature or electrical current input as the control parameter. The design approach to a bias spring SMA actuation element described herein will produce a practical and convenient

method. It is also useful in the design of other types of SMA bias force actuator that use the spring or similar structures (for example elastic beams) to generate the restoring force.

Reference

[1] Deshpande V.S., Fleck N.A. and Ashby M.F., "Effective properties of the octet-truss lattice material", J. Mech. Phys. Solids, Vol. 49, 2001, pp.1724-1769.

[2] Evans A.G. Hutchinson J.W., Fleck N.A., Ashby M.F. and Wadley H.N.G., "The topological design of multifunctional cellular metals", Prog. Mater. Sci., Vol. 46, 2001, pp309-327.

[3] Wicks N. and Hutchinson J.W., "Optimal truss plates", Int. J. Solids and Structures, Vol.38, 2001, pp5165-5183.

[4] Lu T.J., Hutchinson J.W. and Evans A.G., "Optimal design of a flexural actuator", Journal of the Mechanics and Physics of Solids, Vol. 49, 2001, pp2071-2093.

[5] Lu T.J. and Evans A.G., "Design of a high authority flexural actuator using an electro-strictive polymer", Sensors and Actuators A, Vol. 99, 2002, pp290-296.

[6] Brinson, L.C., "One-dimensional constitutive behavior of shape memory alloys: thermomechanical derivation with non-constant material functions and refined martensite internal variable ", J. Intelligent Material Systems and Structures, Vol. 4, 1993, pp.229-242.

[7] Carslaw, H.S., Jaeger, J.C., Conduction of Heat in Solids, Oxford University Press, Oxford, 1959.

[8] Juvinall R.C. and Marshek K.M., Fundamentals of Machine Component Design, Wiley, New York, 1999.

[9] Ashby M.F., Materials Selection in Mechanical Design, Pergamon Press, Oxford,1992.

[10] Allen H.G., Analysis and Design of Structural Sandwich Panels, Pergamon Press, Oxford, 1969.

[11] Zenkert D., An Introduction to Sandwich Construction, Warley, West Midlands, 1995.

[12] Aird T.J., and J.R. Rice, "Systematic search in high dimensional sets", SIAM Journal on Numerical Analysis, Vol. 14, 1977, pp296-312.

L H Han
Department of Engineering
University of Cambridge
Trumpington Street
Cambridge CB2 1PZ
United Kingdom
Tel. Int + 44 1223 332 609
Fax. Int + 44 1223 332 662
E-mail: lhh24@eng.cam.ac.uk